CMLS, Cell. Mol. Life Sci. 60 (2003) 1575–1580
1420-682X/03/081575-06
DOI 10.1007/s00018-003-3171-z

CMLS Cellular and Molecular Life Sciences

Lipid interactions with transmembrane proteins

D. Marsh

Max-Planck-Institut für biophysikalische Chemie, Abt. Spektroskopie, 37070 Göttingen (Germany),
Fax: + 49 551 201 1501, e-mail: dmarsh@gwdg.de.

Abstract. Magnetic resonance results, principally from ^{2}H-nuclear magnetic resonance, indicate that the mean lipid-chain ordering at the surface of transmembrane proteins is comparable to that in fluid lipid bilayers. Principally, it is the requirement for matching the hydrophobic lengths of lipid and protein that modulates the degree of chain ordering at the lipid-protein interface. The distribution of chain order parameters is, nonetheless, broader in the presence of integral proteins than in fluid lipid bilayers. The chain configurations of the phospholipids that are resolved in crystals of integral membrane proteins display considerable conformational heterogeneity. Chain C–C dihedral angles are, however, not restricted to the energetically allowable *trans* and *gauche* rotamers. This indicates that the chains of a given lipid do not have a unique configuration in protein crystals.

Key words. Chain conformation; *trans-gauche* isomerism; order parameter; crystal structures; cytochrome oxidase; phosphatidylethanolamine.

Introduction

It goes without saying that interactions with the membrane lipids are essential to the structure and stability of integral proteins. A considerable amount of information on the lipid-protein interactions in fully hydrated, fluid membranes has been obtained from magnetic resonance studies [1–4]. More recently, the configuration of lipid molecules associated with integral membrane proteins in crystals has been resolved by X-ray diffraction [5, 6].

The purpose of this short review is to compare and contrast the results on lipid-protein interactions obtained by magnetic resonance and x-ray crystallography. Chain conformation and ordering in lipid membranes is reviewed first. This is followed by a discussion of pertinent results on lipid interactions with transmembrane proteins derived from magnetic resonance measurements. Finally, the configuration of phospholipids in membrane protein crystals is addressed.

Lipid-chain conformation and orientation

Lipid-chain conformations in membranes are governed by the torsional potential about the individual C–C bonds of the chain backbone, together with longer-range steric interactions that arise from coupled rotations about two or more backbone C–C bonds [7, 8]. There are three stable rotamers about an sp^3 C-C bond: *trans* (*t*), *gauche*$^+$ (g^+) and *gauche*$^-$ (g^-) with dihedral angles 180° and ca. ±60°, respectively (see fig. 1). The *gauche* conformers lie approximately 0.5 kcal/mol in internal energy above the *trans* conformer. The energy barrier between *trans* and *gauche* is approximately 3 kcal/mol; that between *gauche*$^+$ and *gauche*$^-$ is prohibitively high. Only *cis* double bonds have a dihedral angle of 0°. The longer-range steric interactions suppress $g^{\pm}g^{\mp}$ conformations about adjacent C–C single bonds. In fluid membranes, other combinations of *gauche* conformations, e. g. $g^{\pm}g^{\pm}$, may also be disfavoured for intermolecular steric reasons [9]. At the lipid protein interface, *gauche* conformations of the lipid chains may be needed to adapt the lipid chain to the protein surface, so as to optimise hydrophobic van der Waals contacts.

The orientation of a given chain segment in the membrane is specified both by the ordering of the chain long axis, *Z*, and by the orientation of the chain segment, *z′*, relative to the long axis. The long-axis ordering is described by an order parameter:

$$S_{ZZ} = \frac{1}{2}\langle 3\cos^2\theta_Z - 1\rangle \qquad (1)$$

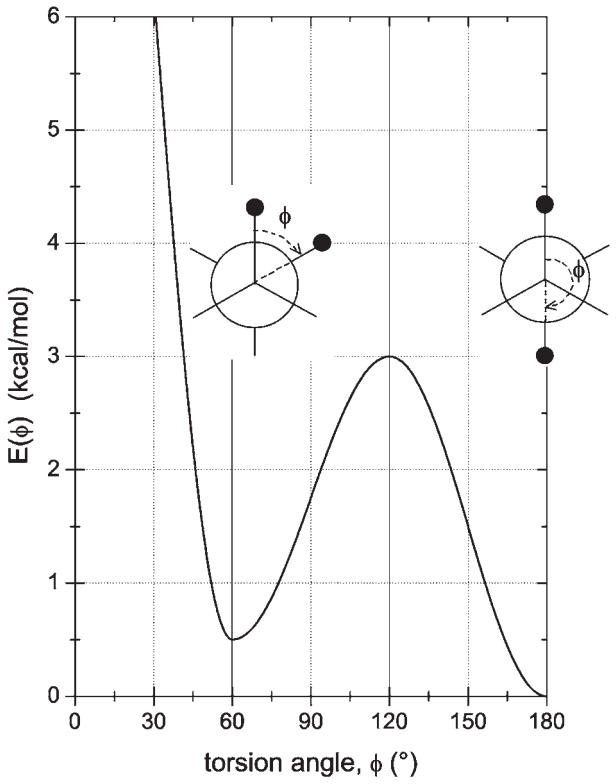

Figure 1. Schematic dependence of C–C bond rotational potential, E(ϕ), on dihedral angle, ϕ. *Trans* (ϕ = 180°) and *gauche*$^+$ (ϕ = 60°) rotamers are indicated as projections along the C–C bond.

where θ_Z is the tilt of the long axis to the membrane normal, and the angular brackets indicate an ensemble or time average. The local segmental ordering, $S_{z'z'}$, is characterised by a limited number of distinct orientations that are determined by the tetrahedral geometry of a C–C bond. These allowed configurations can be designated by the local bond conformation (*trans* or *gauche*$^\pm$), together with the orientation (0°, 60° or 90°) of the segment axis relative to the long axis of the all-*trans* chain (see e.g. ref. [8]). Table 1 gives typical experimental data for various chain segments of phosphatidylcholine in fluid lipid membranes (see [10]). These data are deduced from measurements of the nuclear magnetic resonance (NMR) order parameters for specifically deuterated chain segments.

In the fluid phase of lipid membranes, there is an extremely rapid interconversion between the different chain conformers, and this is accompanied by rapid fluctuations in orientation of the chain long axis. For lipids associated with the protein surface, conformational and orientational transitions will, in general, be slower. Ultimately, they may be determined by the residence time of the lipid at a particular site on the protein surface.

Magnetic resonance results on lipid-protein interactions

Spin-label ESR

Because the motional timescale is favourable, electron spin resonance (ESR) spectroscopy can resolve spin-labelled lipids that interact directly with the transmembrane sections of integral proteins. This has enabled extensive studies on the stoichiometry and selectivity of lipid interactions with a wide variety of integral membrane proteins (see [4], for a review). The lipid stoichiometry correlates with the intramembranous perimeter of the protein that is exposed to the hydrophobic membrane milieu. The lipid headgroup specificity exhibits selectivity of interaction with certain of the protein residues. Protein-interacting spin-labelled lipids are distinguished spectroscopically in ESR principally by the slowing of chain rotational motion – a result that is confirmed by NMR measurements [11]. Information about chain orientation and ordering can be obtained from ESR measurements with macroscopically aligned samples [12]. This has been done for oriented rod outer segment discs: it was found that there is a wide orientational distribution, i.e. a considerable degree of disorder, of the lipid chain segments associated with the visual receptor rhodopsin [13].

^{2}H-NMR

The range of motional sensitivity of ^{2}H-NMR is such that exchange on and off the protein averages the spectra from deuterated lipids in these two environments. Spin-label ESR measurements put lipid residence times on the protein in the microsecond region [4, 14]. Quadrupolar ^{2}H-

Table 1. Lipid-chain conformation and ordering in dimyristoyl phosphatidylcholine membranes in the fluid phase (T = 40 °C) [10].

Chain segment	Order parameters[a]		Conformational population[b]		
	S_{ZZ}	$S_{z'z'}$	$p(t,0°)$	$p(g^\pm,60°)$	$p(g^\pm,90°)$
C-6	0.50	0.74	0.80	0.20	0.00
C-10	0.50	0.56	0.66	0.28	0.06
C-13	0.50	0.35	0.51	0.36	0.13

[a] S_{ZZ} is the principal order parameter of the chain long axis; $S_{z'z'}$ is the principal order parameter of the chain segment.
[b] Chain configurations are characterised by the conformation (*trans*, *gauche*$^\pm$) relative to the previous segment, and by the orientation (0°, 60°, 90°, 120° or 180°) of the segment axis relative to the initial *trans* segments (see e.g. [8]).

Table 2. Order parameter (S_{mol}) distribution of perdeuterated dimyristoyl phosphatidylcholine ($diC_{14}PC$) chains in rhodopsin-containing $diC_{14}PC$ membranes of different lipid/protein ratios, in the fluid phase ($T = 23\,°C$) [17].[a]

L/P (mol/mol)	$\langle S_{mol}\rangle$	$[\langle S_{mol}^2\rangle - \langle S_{mol}\rangle^2]^{1/2}$
∞	0.19	± 0.06
150:1	0.19	± 0.08
50:1	0.15	± 0.08
30:1	0.15	± 0.11
12:1	0.18	± 0.14

[a] $\langle S_{mol}\rangle$ is the mean order parameter of the different chain segments ($S_{mol} = S_{ZZ}S_{z'z'}$) and $\langle S_{mol}^2\rangle - \langle S_{mol}\rangle^2 = \langle (S_{mol} - \langle S_{mol}\rangle)^2\rangle$ is the mean squared width of the order parameter distribution.

NMR spectra therefore reflect the ensemble or time-average chain order in the entire membrane. A general feature found from such measurements is that the orientational order of the lipid chains at the protein interface is not greatly dissimilar from that in fluid lipid bilayer membranes [15, 16]. Results obtained for rhodopsin reconstituted in lipid membranes with perdeuterated chains are given in table 2. The mean chain order parameter, $\langle S_{mol}\rangle$, decreases slightly with increasing protein content. For specifically deuterated phosphatidylcholines interacting with the myelin proteolipid protein, the lipid chain order parameter changes hardly at all [11]. An interesting feature of the data presented in table 2 is that although the mean order parameter changes relatively little, the spread of chain order parameters increases progressively with increasing protein concentration in the membrane. This can be attributed variously to the irregular intramembranous surface of the protein and to a statistical heterogeneity in protein-lipid contacts (on the ^{2}H-NMR timescale) – see Bienvenue et al. [17].

A comparable degree of chain ordering at the protein interface and in fluid bilayer regions of the membrane implies that configurational entropy does not contribute strongly to the energetics of lipid-protein interaction. It also implies good hydrophobic matching between the lipid chains and the transmembrane domains of the protein. For this reason, matching of lipid chain order becomes a crucial energetic requirement for optimal integration of the protein into the membrane. Table 3 shows the effect on lipid order of varying the relative hydrophobic thicknesses of transmembrane peptides and the lipid bilayer. Lipid chains that are shorter than the hydrophobic span of the peptide become more ordered (or extended), whereas those that are longer become more disordered (or compressed), than in bilayers without peptide. Hydrophobic matching is an essential determinant of acyl chain order at the protein-lipid interface.

Table 3. Increase, $\Delta\langle S_{mol}\rangle$, in mean order parameter of perdeuterated phosphatidylcholine (diC_nPC) chains on membrane incorporation of 1:30 mol/mol of transmembrane peptide [18].[a]

Peptide	$diC_{12}PC$	$diC_{14}PC$	$diC_{16}PC$	$diC_{18}PC$
$AW_2(LA)_5W_2A$	+0.05	+0.03	+0.00	–0.02
$AW_2(LA)_5LW_2A$	+0.09	+0.03	+0.01	–0.01
$AW_2(LA)_6LW_2A$	+0.12	+0.04	+0.01	+0.00
gramicidin A	+0.13	+0.07	+0.02	–0.01

[a] Measurements are made 10° above the chain-melting temperature of the respective lipid bilayers.

Crystals of Integral Membrane Proteins

Certain crystal structures of transmembrane proteins in the Protein Data Base now contain some associated phospholipids. Those lipids that are well resolved crystallographically by no means correspond to complete coverage of the hydrophobic protein surface. It is therefore appropriate to enquire whether these are special lipids or are generally representative of the lipids that surround integral proteins in fully hydrated fluid membranes.

Here we look at the 12 phosphatidylethanolamine molecules that are associated with the two monomers of the four-subunit cytochrome *c* oxidase from *Rhodobacter sphaeroides* [19] – see figure 2. This dataset allows comparison of an appreciable number of independent lipids. It yields results that are fairly representative of aggregate values obtained from the more limited number of lipids resolved in the crystal structures of a variety of transmembrane proteins [D. Marsh and T. Pàli, unpublished results].

Glycerol backbone configuration

The dihedral angles with respect to the pendant groups of the glycerol backbone, θ_4 and θ_2, specify the relative orientations of the *sn*-1 and *sn*-2 chains and the orientation of the headgroup relative to the *sn*-2 chain, respectively. *Gauche* rotations for θ_4 allow parallel chain stacking, and they are also favoured internally for both θ_4 and θ_2 (the '*gauche* effect') [21].

Of the six distinguishable phosphatidylethanolamine molecules associated with *Rb. sphaeroides* cytochrome oxidase, only half have the energetically allowed staggered conformations of the glycerol backbone. One molecule of these (PEH 2009) has an optimal $\theta_4/\theta_2 = g^+g^-$ configuration with parallel chain stacking. The PEH 2010 lipid has a $\theta_4/\theta_2 = g^+t$ combination with parallel chain stacking, and PEH 2011 has a $\theta_4/\theta_2 = tg^+$ combination with nonparallel chain stacking. Eclipsed conformations for the glycerol backbone (lipids: PEH 2008, PEH 2012 and PEH 2013) are energetically forbidden for the isolated phospholipid molecule and presumably correspond to conformational heterogeneity of these lipids associated with cytochrome oxidase in the crystals.

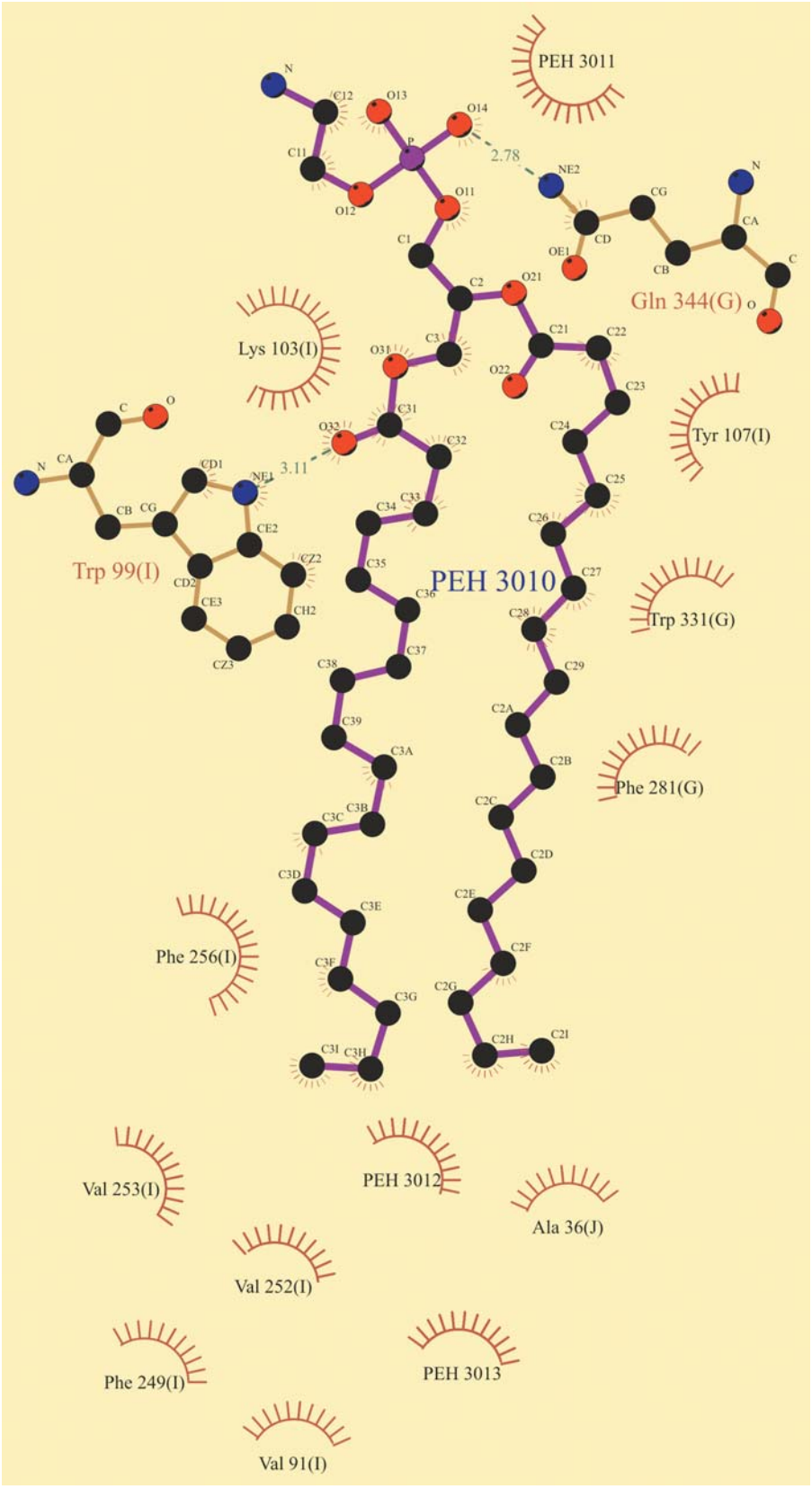

Figure 2. Distearoyl phosphatidylethanolamine (diC_{18}PE) in association with cytochrome *c* oxidase from *R. sphaeroides* (PDB: 1M56; [19]). LIGPLOT diagram [20] shows neighbouring protein residues and diC_{18}PE molecules (PEH 3011-3) that are involved in hydrophobic contacts. Hydrogen bonds are indicated explicitly.

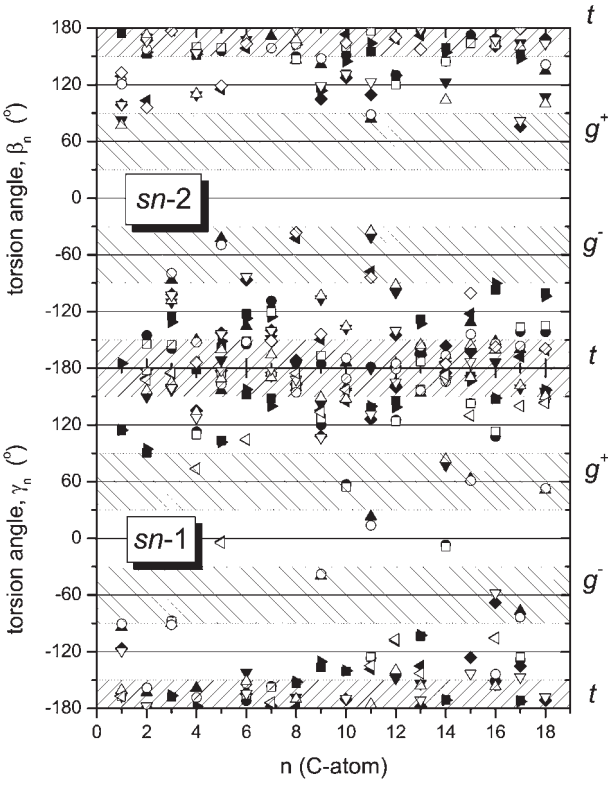

Figure 3. Torsion angles, $C_{n-3}C_{n-2}C_{n-1}C_n$, in the *sn*-1 (γ_n, lower panel) and *sn*-2 (β_n, upper panel) chains of $diC_{18}PE$ in crystals of *Rb. sphaeroides* cytochrome *c* oxidase (PDB: 1M56; [19]). Different symbols correspond to the 12 molecules of $diC_{18}PE$. Dihedral angles are given as a function of position, C_n, in the chain. The allowed *trans* (*t*) and *gauche*$^{\pm}$ ($g^{\pm}$) conformers are indicated by shading.

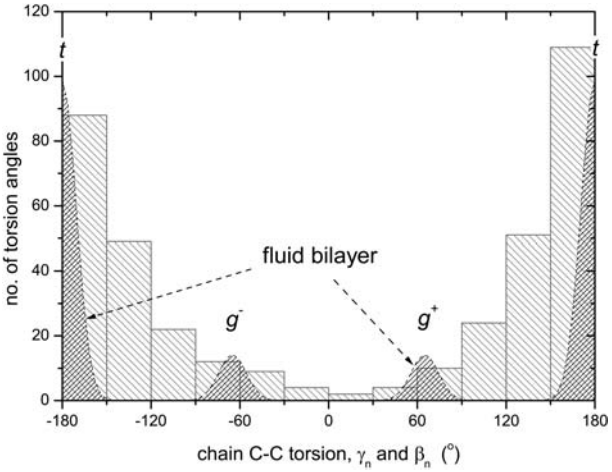

Figure 4. *Histogram*: Distribution of C–C torsion angles in the *sn*-1 and *sn*-2 chains from 12 $diC_{18}PE$ molecules in *Rb. sphaeroides* cytochrome *c* oxidase crystals (PDB:1M56; [19]). *Dashed lines*: Distribution of chain torsion angles in fluid lipid bilayer membranes of $diC_{14}PC$ from molecular dynamics simulations [22].

Chain Configuration

Figure 3 gives the torsion angles, γ_n and β_n, in the *sn*-1 and *sn*-2 chains, respectively, of the distearoyl phosphatidylethanolamine molecules in crystals of *Rb. sphaeroides* cytochrome *c* oxidase. The torsion angles γ_2 and β_2 represent the ester carboxyl group and therefore should be in the *trans* conformation. It is seen from figure 3 that not all acyl chain structures fulfil the requirement for planar carboxyl groups. In particular, lipids PEH 2008/3008 and PEH 2013/3013 have values of γ_2 and β_2, respectively, that are much less than 180°.

Torsion angles γ_n, β_n with $n \geq 3$ represent the configuration of the lipid hydrocarbon chains. One therefore expects that γ_n, $\beta_n \approx 180°$ or $\pm 60°$, corresponding to *trans* and *gauche* rotamers, respectively. A value of γ_n, $\beta_n \approx 0°$ should represent a *cis* double bond. The chain segments in Fig. 3 are predominantly in the *trans* conformation, for both the *sn*-1 and *sn*-2 chains. The proportion of *gauche* conformations is considerably smaller. On the whole, the *gauche* conformers are not strongly correlated and mostly are associated with adjacent *trans* sequences. There is one g^-g^- configuration and one g^-tg^- configuration in the *sn*-2 chains. A classical g^+tg^- kink sequence occurs towards the end of one *sn*-1 chain, and is combined with a g^-g^+ sequence that is allowed only at the chain end. *Cis* configurations are found solely in the *sn*-1 chains, although chain unsaturation commonly occurs at the *sn*-2 position of membrane glycerolipids. Where found, the *cis*-configurations are not invariably associated with neighbouring *gauche* conformations, nor with adjacent *skew* (~120° dihedrals) conformations that achieve quasi straight-chain packing with *cis* double bonds.

Figure 4 shows the distribution of lipid-chain torsion angles in cytochrome oxidase crystals. The torsion-angle distribution obtained from a molecular dynamics simulation of fluid lipid bilayers is included for comparison. As seen from figure 4, the chain disorder of the phosphatidylethanolamine lipids in cytochrome oxidase crystals is associated primarily not with *gauche* rotamers but with the disfavoured anticlinal (γ_n, $\beta_n = 120°$) conformers. Such configurations for a polymethylene chain would carry an extremely high energy penalty (see fig. 1). This suggests that torsion angles in the $120 \pm 30°$ range in fact represent conformational heterogeneity of the lipid chains, which remains unresolved in the electron density maps from the protein crystals. Molecular dynamics simulations for fluid lipid bilayers (see fig. 4) support this interpretation – chain segments with 120° torsion angles are not found [22]. Of particular relevance also is the fact that the B-values of the lipids in membrane protein crystals are appreciably higher than those for the protein [D. Marsh and T. Palí, unpublished results].

Conclusions

Conformational violations of the type described above are not atypical for the structures of lipids in crystals of

transmembrane proteins [D. Marsh and T. Palí, unpublished results]. Configurational disorder and heterogeneity appear to be general features of protein-interacting lipids in crystals. At this level, the crystallographically resolved lipids share properties in common with those of the dynamically disordered lipids in fully hydrated fluid membranes that have been investigated by magnetic resonance methods. Quantitative comparisons should perhaps await better resolution. But this, of course, begs the question whether the lipids that are not resolved crystallographically possess a higher degree of configurational disorder. The six unique lipids resolved in crystals of *Rb. sphaeroides* cytochrome oxidase are located at well-defined positions, in a cleft formed by the two-helix bundles of subunit III, or at the interface between subunit IV and subunits I/III [19]. Adaptation of the lipid configuration to the protein surface is, of course, an essential requirement for good hydrophobic matching.

1 Jost P. C. and Griffith O. H., eds (1982) Lipid-Protein Interactions, vol. 2, Wiley-Interscience, New York
2 Watts A. and de Pont J. J. H. H. M., eds (1985) Progress in Protein-Lipid Interactions, vol. 1, Elsevier, Amsterdam
3 Watts A., Ed. (1993) New Comprehensive Biochemistry, vol. 25, Elsevier, Amsterdam
4 Marsh D. and Horváth L. I. (1998) Structure, dynamics and composition of the lipid-protein interface. Perspectives from spin-labelling. Biochim. Biophys. Acta **1376:** 267–296
5 Fyfe P. K., McAuley K. E., Rothmann M., Isaacs N. W., Cogdell R. J. and Jones M. R. (2001) Probing the interface between membrane proteins and membrane lipids by x-ray crystallography. Trends Biochem. Sci. **26:** 106–112
6 Pebay-Peyroula E. and Rosenbusch J. P. (2001) High-resolution structures and dynamics of membrane protein-lipid complexes: a critique. Curr. Opin. Struct. Biol. **11:** 427–432
7 Flory P. J. (1969) Statistical Mechanics of Chain Molecules, Wiley, London
8 Cevc G. and Marsh D. (1987) Phospholipid Bilayers. Physical Principles and Models, Wiley-Interscience, New York
9 Marsh D. (1974) Statistical mechanics of the fluidity of phospholipid bilayers and membranes. J. Membrane Biol. **18:** 145–162
10 Moser M., Marsh D., Meier P., Wassmer K.-H., and Kothe G. (1989) Chain configuration and flexibility gradient in phospholipid membranes. Comparison between spin-label electron spin resonance and deuteron nuclear magnetic resonance, and identification of new conformations. Biophys. J. **55:** 111–123
11 Meier P., Sachse J.-H., Brophy P. J., Marsh D., and Kothe G. (1987) Integral membrane proteins significantly decrease the molecular motion in lipid bilayers: a deuteron NMR relaxation study of membranes containing myelin proteolipid apoprotein. Proc. Natl. Acad. Sci. USA **84:** 3704–3708
12 Marsh D. (1983) Spin label answers to lipid-protein interactions. Trends Biochem. Sci. **8:** 330–333
13 Pates R. D. and Marsh D. (1987) Lipid mobility and order in bovine rod outer segment disk membranes. A spin-label study of lipid-protein interactions. Biochemistry **26:** 29–39
14 Horváth L. I., Brophy P. J., and Marsh D. (1993) Exchange rates at the lipid-protein interface of the myelin proteolipid protein determined by saturation transfer electron spin resonance and continuous wave saturation studies. Biophys. J. **64:** 622–631
15 Seelig J., Seelig A., and Tamm L. (1982) Nuclear magnetic resonance and lipid-protein interactions. In: Lipid-Protein Interactions, vol. 2, pp. 127–148, Jost P. C. and Griffith O. H. (eds), John Wiley, New York
16 Bloom M. and Smith I. C. P. (1985) Manifestations of lipid-protein interactions in deuterium NMR. In: Progress in Protein-Lipid Interactions, vol. 1, pp. 61–88, Watts A. and de Pont J. J. H. H. M. (eds), Elsevier, Amsterdam
17 Bienvenue A., Bloom M., Davis J. H., and Devaux P. F. (1982) Evidence for protein-associated lipids from deuterium nuclear magnetic resonance studies of rhodopsin-dimyristoylphosphatidylcholine recombinants. J. Biol. Chem. **257:** 3032–3038
18 de Planque M. R. R., Greathouse D. V., Koeppe R. E. II, Schäfer H., Marsh D., and Killian J. A. (1998) Influence of lipid/peptide hydrophobic mismatch on the thickness of diacylphosphatidylcholine bilayers. A ^{2}H NMR and ESR study using designed transmembrane α-helical peptides and gramicidin A. Biochemistry **37:** 9333–9345
19 Svensson-Ek M., Abramson J., Larsson G., Törnroth S., Brzezinski P., and Iwata S. (2002) The X-ray crystal structures of wild-type and EQ(I-286) mutant cytochrome *c* oxidases from *Rhodobacter sphaeroides*. J. Mol. Biol. **321:** 329–339
20 Wallace A. C., Laskowski R. A., and Thornton J. M. (1995) LIGPLOT – a program to generate schematic diagrams of protein ligand interactions. Prot. Engin. **8:** 127–134
21 Pascher I., Lundmark M., Nyholm P.-G. and Sundell S. (1992) Crystal structures of membrane lipids. Biochim. Biophys. Acta **1113:** 339–373
22 Róg T. and Pasenkiewicz-Gierula M. (2001) Cholesterol effects on the phosphatidylcholine bilayer nonpolar region: a molecular simulation study. Biophys. J. **81:** 2190–2202